

Does A Relationship Between Arctic Low Clouds and Sea Ice Matter?

Patrick C. Taylor^{1, a)}

¹*NASA Langley Research Center, 21 Langley Blvd. Hampton, VA, USA 23602*

^{a)}*Corresponding author: patrick.c.taylor@nasa.gov*

Abstract. Arctic low clouds strongly affect the Arctic surface energy budget. Through this impact Arctic low clouds influence important aspects of the Arctic climate system, namely surface and atmospheric temperature, sea ice extent and thickness, and atmospheric circulation. Arctic clouds are in turn influenced by these elements of the Arctic climate system, and these interactions create the potential for Arctic cloud-climate feedbacks. To further our understanding of potential Arctic cloud-climate feedbacks, the goal of this paper is to quantify the influence of atmospheric state on the surface cloud radiative effect (CRE) and its covariation with sea ice concentration (SIC). We build on previous research using instantaneous, active remote sensing satellite footprint data from the NASA A-Train. First, the results indicate significant differences in the surface CRE when stratified by atmospheric state. Second, there is a weak covariation between CRE and SIC for most atmospheric conditions. Third, the results show statistically significant differences in the average surface CRE under different SIC values in fall indicating a 3-5 W m⁻² larger LW CRE in 0% versus 100% SIC footprints. Because systematic changes on the order of 1 W m⁻² are sufficient to explain the observed long-term reductions in sea ice extent, our results indicate a potentially significant amplifying sea ice-cloud feedback, under certain meteorological conditions, that could delay the fall freeze-up and influence the variability in sea ice extent and volume. Lastly, a small change in the frequency of occurrence of atmosphere states may yield a larger Arctic cloud feedback than any cloud response to sea ice.

INTRODUCTION

Climate change in the Arctic is outpacing the rest of the globe and Arctic Ocean sea ice melting is the most visible sign. Microwave radiometer data since 1979 indicate that September sea ice extent has decreased by about 13% per decade (Cavalieri et al. 1996). Climate model projections of Arctic sea ice extent indicate that the first ice-free Arctic summer could be as early as the 2030s or as late as the 2080s (Snape and Forster 2014). The rate at which sea ice retreat occurs depends upon a number of factors such as atmospheric wind patterns, sea ice dynamics, ocean circulation, and influences on the surface radiation budget—e.g., melt ponds, snow cover, and sea ice age influencing surface albedo and clouds, atmospheric temperature, and water vapor influencing downwelling longwave radiation (Kwok and Untersteiner 2011).

Arctic clouds, especially low clouds, have a strong influence on the surface energy budget (e.g., Curry et al. 1996; Kay and L’Ecuyer 2013). Through this impact, Arctic clouds influence important aspects of the Arctic climate, namely surface and atmospheric temperature, sea ice extent and thickness, and atmospheric circulation. Analyzing the annual cycle of CRE, Arctic clouds warm the surface most of the year by enhancing longwave downwelling radiation to the surface (e.g., Kay and L’Ecuyer 2013). However, Arctic clouds cool the surface during the summer. Several papers indicate that in winter the presence or absence of clouds results in two different Arctic surface radiative flux regimes where in the presence of clouds the net longwave surface flux is near-zero whereas in the absence of clouds the Arctic surface experiences a strong radiative cooling of more than -30 Wm⁻² (Morrison et al. 2012). This result demonstrates the importance of clouds to the Arctic surface radiation budget and in sea ice extent and volume. It further underscores the importance of understanding the factors (e.g., atmospheric dynamics, thermodynamics, sea ice, etc.) that most strongly influence the CRE (Taylor 2012; Taylor et al. 2013).

Accumulating evidence suggests an autumn cloud response to reduced sea ice extent, however the radiative impact on the surface energy budget of this potential feedback is unknown. The radiative impact of clouds on the surface radiation budget is defined here using the conventional definition of surface CRE as the difference between

all- and clear-sky fluxes (e.g., Boeke and Taylor 2016). The goal of this paper is to quantify the radiative impact of the covariation between clouds and sea ice demonstrated by Taylor et al. (2015) by addressing two questions. (1) Does the surface CRE vary with atmospheric state? (2) Does the surface CRE change with sea ice conditions?

DATA

Surface radiative flux and sea ice concentration (SIC) data (Cavalieri et al. 1996) are taken from the Ed RalB1 RalB1 CALIPSO-CloudSat-CERES-MODIS (C3M) data extending from July 2006 through June 2010 (Kato et al. 2011). C3M provides vertical profiles of cloud properties including cloud fraction and cloud liquid and ice water content. Cloud properties are taken from the merged satellite radar-lidar retrievals averaged over 20 km CERES footprints. The C3M merging process collocates Cloud-Aerosol Lidar with Orthogonal Polarization (CALIOP) version 3 Vertical Feature Mask (30 m vertical resolution below 8.2 km; Winker et al., 2007), CloudSat Cloud Profiling Radar (CPR; Stephens et al., 2008) CLDCLASS product (240 m vertical resolution) (Sassen and Wang 2008), Clouds and Earth's Radiant Energy System (CERES; Wielicki et al. 1996), and Aqua Moderate Resolution Imaging Spectrometer (MODIS) onto the CERES footprint. The C3M cloud property profiles have a vertical resolution of 120 m. Footprint averaged clear- and all-sky surface radiative fluxes are computed using the Langley modified Fu-Liou radiative transfer model (Kato et al. 2005), the C3M derived cloud field, and atmospheric state from data assimilation. Figure 2 in Kato et al. (2011) indicates that using CALIPSO and CloudSat derived cloud properties significantly improves the agreement of computed TOA LW irradiance with CERES over the Arctic in January and July. Lastly, atmospheric state information important for the methodology described below is taken from the Modern Era Retrospective analysis for Research and Applications (MERRA; Rienecker et al. 2011).

METHODOLOGY

Atmospheric Regimes

The Arctic is separated into four atmosphere regimes based upon lower tropospheric stability (LTS) and 500 hPa vertical velocity (ω_{500}) following Barton et al. (2012). LTS is defined as the difference between the potential temperature at 700 hPa (θ_{700}) and the surface (θ_{SFC}): $LTS = \theta_{700} - \theta_{SFC}$. Three of the states differ only by LTS, namely stable (S; $LTS < 16$ K), highly stable (HS; $16 \text{ K} < LTS < 24 \text{ K}$), and very highly stable (VHS; $LTS > 24 \text{ K}$) and are characterized by weak mid-tropospheric subsidence ($\omega_{500} > -8.6 \text{ hPa day}^{-1}$). The fourth atmospheric regime, uplift regime (UL), is defined by mid-tropospheric rising motion ($\omega_{500} < -8.6 \text{ hPa day}^{-1}$) and any LTS value. Each footprint is placed into an atmospheric regime by collocating it with the closest MERRA grid point in space and time.

Compositing Approach

Previous investigations into the relationship between clouds and sea ice are conducted at the monthly average and gridded scales. Two weaknesses with this approach are that (1) clouds respond quickly to their environment and therefore the signal in the monthly average is likely to be weaker and (2) monthly averaged data makes it difficult to deconvolve the influence of meteorology from that of sea ice.

We follow the approach of Taylor et al. (2015) using instantaneous satellite footprint data to construct composites within seven SIC bins and the four atmospheric state regimes. First, each footprint is placed into one of the four defined atmospheric state regimes. Second, each footprint is placed within a SIC bin. Lastly, the average is taken for each surface CRE within each atmospheric regime and SIC bin. Covariation between a variable and SIC is assessed using the statistically significant difference (95% confidence) between the mean values across the SIC bins.

As in Taylor et al. (2015), the computation of regional anomalies within each atmospheric regime is necessary to consider the domain-averaged response. This is because there is a regional variability in the average cloud properties and radiative effect within each atmospheric regime. In other words, the cloud properties found in the HS regime over the Beaufort Sea are statistically different from the cloud properties in the HS regime occurring over the North Atlantic because the large-scale meteorological conditions that generate the HS regime differ between the regions.

RESULTS

There is a strong dependence of the surface CRE on atmospheric state regime. Table 1 summarizes the domain-averaged values of surface CRE in three seasons defined by Taylor et al. (2015). Considering the regimes only separated by LTS, a consistent result is found in all seasons where the magnitude of the CRE, both LW and SW, is larger at smaller LTS values. This result is consistent with the larger cloud fraction and cloud liquid water path found at smaller LTS values (Taylor et al. 2015). Strong seasonal variability in the LW CRE is found within individual atmospheric state regimes. The S regime exhibits the weakest seasonal variations in LW CRE and varies between 53-60 W m^{-2} . The HS and VHS regimes show a stronger seasonality, however with slightly different behavior. Both HS and VHS regimes show the smallest LW CRE during winter; however, HS shows a larger LW CRE during fall than summer whereas VHS exhibits a weaker LW CRE during fall than summer. Strong seasonal variability in SW CRE is also found, however primarily determined by the seasonality of solar insolation.

TABLE 1. Arctic domain average surface cloud radiative effects by season and atmospheric state regime. All units are W m^{-2} .

Months with zero solar insolation have a 0 W m^{-2} SW CRE.

Atmospheric Regime	Summer (JJA)		Fall (SO)		Winter (NDJFMAM)	
	LW CRE	SW CRE	LW CRE	SW CRE	LW CRE	SW CRE
VHS (LTS >24 K)	40.6	-57.5	37.9	-10.8	24.4	-8.1
HS (16<LTS<24 K)	50.1	-70.1	53.0	-16.6	37.9	-11.8
S (LTS<16 K)	55.7	-80.8	59.5	-20.2	53.6	-19.7
UL ($\omega_{500} < -8.6 \text{ hPa day}^{-1}$)	51.8	-85.1	56.6	-22.3	48.6	-18.6

Figures 1 and 2 summarize the average values of the surface LW and SW CRE as a function of SIC. Generally speaking the surface LW CRE becomes less positive and surface SW CRE becomes less negative at larger SIC. The magnitude of the LW CRE-SIC relationship indicates that LW CRE is 3 to 5 W m^{-2} larger for 0% SIC than for 100% SIC footprint in fall. Note that clouds are not solely responsible for the LW and SW CRE dependence on SIC, because as defined air and surface temperature, humidity and surface albedo changes also influence CRE. Further analysis is required to unscramble these individual contributions and isolate the cloud effect.

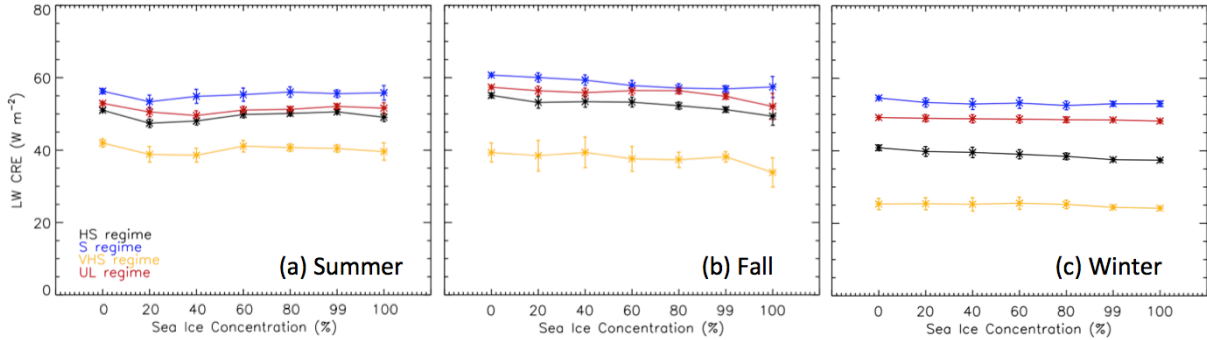


FIGURE 1. Average surface LW CRE composited by SIC for each atmospheric regime and season: (a) summer, (b) fall, and (c) winter. Error bars represent the 2σ standard error for each average. Each bin is plotted by the upper SIC limit.

The SW CRE results are plotted assuming a constant surface albedo to account for the change in surface albedo with SIC. In summer, the result suggests a potential 10-15 W m^{-2} decrease in the SW CRE between open ocean and completely sea ice covered scenes. The “sine-like” pattern in both Fig. 1a and 2a is due to the variation of cloud liquid water path with SIC (Taylor et al. 2015). The differences shown (Fig. 2) are not statistically significant and more samples are required to reduce noise and constrain the potential feedback.

CONCLUSION

Arctic clouds, especially low clouds, strongly influence surface and atmospheric energy budgets. This paper investigates several factors the influence the surface CRE: namely, atmospheric conditions and SIC. The results show that (1) atmosphere state is a significant and the primary control on the surface CRE. (2) There is a weak covariability between CRE and SIC for most atmospheric regimes during summer and winter. (3) Statistically

significant differences are found in the average surface CRE under different SICs in autumn. Under the HS regime, the results suggest up to a 5 W m^{-2} larger surface LW CRE occurs over open ocean than 100% sea ice cover.

The third conclusion is particularly interesting because the sea ice melt over the past few decades can be explained by a surface energy imbalance of less than 1 W m^{-2} . Thus, this result indicates a potentially significant amplifying sea ice-cloud feedback where under certain meteorological conditions reduced sea ice would contribute to an increased surface LW CRE that could delay the autumn freeze-up and influence sea ice extent and volume. The results also indicate that a shift in the Arctic atmospheric states can yield a larger Arctic cloud feedback than any cloud response to sea ice. In closing a small change in the surface CRE, whether arising from a sea ice change or from a shift in atmospheric circulation and stability, can have significant impact on future sea ice cover.

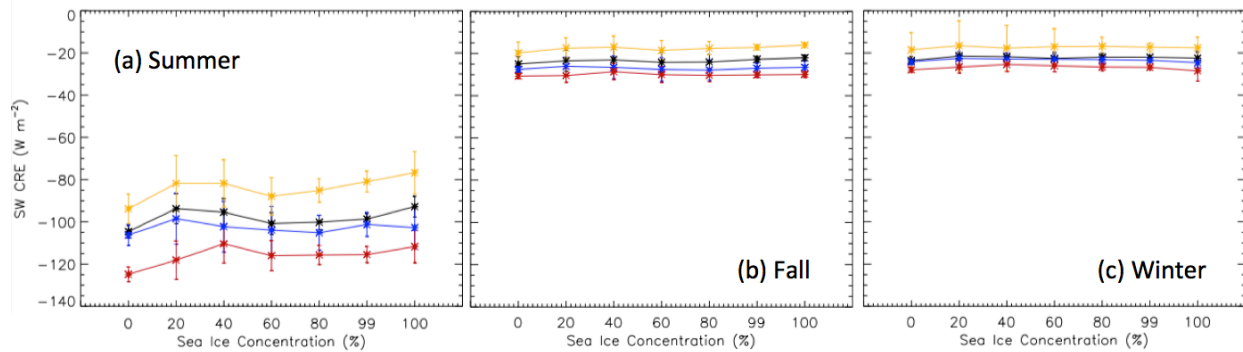


FIGURE 2. Average surface SW CRE (W m^{-2}) composited by SIC for each atmospheric regime and season: (a) summer, (b) fall, and (c) winter. Error bars represent the 2σ standard error for each average. Each bin is plotted by the upper SIC limit.

ACKNOWLEDGMENTS

The author would like to acknowledge that this work is funded by the NASA Interdisciplinary Studies Program grant NNH12ZDA001N-IDS.

REFERENCES

1. D. J. Cavalieri, C. L. Parkinson, P. Gloersen, and H. Zwally, Boulder, Colorado USA: NASA National Snow and Ice Data Center Distributed Active Archive Center. <http://dx.doi.org/10.5067/8GQ8LZQVL0VL> (1996).
2. T. J. Snape and P. M. Forster, Decline of Arctic sea ice: Evaluation and weighting of CMIP5 projections, *J. Geophys. Res. Atmos.*, **119**, 546-554, doi: 10.1002/2013JD020593 (2014).
3. R. Kwok and N. Untersteiner, The thinning of Arctic sea ice, *Phys. Today*, 36-41 (2011).
4. J. A. Curry, W. B. Rossow, D. Randall, and J. L. Schramm, *J. Climate*, **9**, 1731-1762 (1996).
5. J. E. Kay and T. L'Ecuyer, *J. Geophys. Res. Atmos.*, **118**, 7219-7236, doi:10.1002/jgrd.50489 (2013).
6. H. G. Morrison, G. de Boer, G. Feingold, J. Harrington, M. D. Shupe, and K. Sulia, 2012: *Nat. Geosci.*, **5**, 11-17, doi:10.1038/ngeo1332 (2012).
7. P. C. Taylor, *Surv. Geophys.*, 1-9, DOI: 10.1007/s107-12-012-9182-2 (2012).
8. P. C. Taylor, M. Cai, A. Hu, J. Meehl, W. Washington, G. J. Zhang, *J. Climate*, **26**, 7023-7043. doi: <http://dx.doi.org/10.1175/JCLI-D-12-00696.1> (2013).
9. R. Boeke and P. C. Taylor, *J. Climate*, (2016)
10. S. Kato, and coauthors, *J. Geophys. Res.* **116**, D19209, doi: 10.1029/2011JD016050 (2011).
11. D. M. Winker and coauthors, *Bull. Amer. Meteor. Soc.*, 1211-1229 (2010).
12. G. L. Stephens and coauthors, *J. Geophys. Res.*, **113**, D00A18, doi:10.1029/2008JD009982 (2008).
13. K. Sassen and Z. Wang, *Geophys. Res. Lett.*, **35**, L04805, doi:10.1029/2007GL032591 (2008).
14. B. A. Wielicki, B. R. Barkstrom, E. F. Harrison, R. B. Lee III, G. L. Smith, and J. E. Cooper, *Bull. Amer. Meteor. Soc.*, **77**, 853-868 (1996).
15. S. Kato, and N. G. Loeb, *J. Geophys. Res.*, **100**, D07202, doi: 10.1029/2004JD005308 (2005).
16. M. M. Rienecker and coauthors, *J. Climate*, **24**, 3624-3648 (2011).
17. N. P. Barton, S. A. Klein, J. S. Boyle, and Y. Y. Zhang, *J. Geophys. Res.*, **117**, D15205, doi:10.1029/2012JD017589 (2012).